Eur. Phys. J. B **26**, 219–228 (2002)
DOI: 10.1140/epjb/e20020083

THE EUROPEAN PHYSICAL JOURNAL B
EDP Sciences

Quasiperiodically driven Josephson junctions: strange nonchaotic attractors, symmetries and transport

E. Neumann[a] and A. Pikovsky

Department of Physics, University of Potsdam, Am Neuen Palais, PF 601553, 14415, Potsdam, Germany

Received 16 August 2001 and Received in final form 22 January 2002

Abstract. We consider the dynamics of the overdamped Josephson junction under the influence of an external quasiperiodic driving field. In dependence on parameter values either a quasiperiodic motion or a strange nochaotic attractor (SNA) can be observed. The latter corresponds to a resistive state in the current-voltage characteristics while for quasiperiodic motion a finite superconducting current exists for zero voltage. It is shown that in the case of SNA a nonzero mean voltage across the junction can appear due to symmetry breakings. Based on this observation a detailed symmetry consideration of the generalized equation of motion is performed and symmetry conditions ensuring zero mean voltage across the junction are found.

PACS. 05.45.-a Nonlinear dynamics and nonlinear dynamical systems – 85.25.Cp Josephson devices – 74.80.Fp Point contacts

1 Introduction

The transport phenomena in nonlinear systems have received an enormous attention in the last decade. The main nontrivial effect here – appearance of a directed current without directed force – is called ratchet; it has been used to explain mechanisms in molecular motors, electronic transport through superlattices, and the dynamics of Josephson junctions, to name only a few of important examples (see, *e.g.* [1,2] and references therein).

In a typical formulation of the problem, one considers a particle in an one-dimensional spatially periodic potential under periodic and fluctuating forces, and studies the mean velocity of the motion. If only thermal (white) noise is present, merely a diffusive transport can be expected, *i.e.* in average there is no preferred direction of motion of the particle. The question "under which additional requirements a directed motion could be observed" has motivated wide investigations of different mechanisms for ratchets. One way to induce a directed transport in periodic asymmetric potentials is to add a colored Gaussian noise in addition to the white thermal one [3,4]. Directed transport can be induced by other forces as well, provided they permanently keep the system away from the equilibrium state. In particular, purely deterministic dynamics is also able to cause a ratchet. In a deterministically rocked (*i.e.* when an additional space-independent periodic in time force is added) periodic potential without reflection symmetry, one can observe regular and chaotic transport depending on the parameters values [5]. In [6] it has been found that current reversals in deterministic ratchets occur due to a bifurcation from a chaotic to a periodic regime. Recently, rather general considerations [7,8] have shown that ratchets appear due to a broken time-space symmetry [4,9].

An important application of the studies of transport phenomena is the Josephson junction [10]. Its dynamics is described by an equation of motion of a particle in a periodic potential. Here a directed particle current due to a non-zero mean velocity corresponds to a non-zero mean voltage across the junction[1], thus one often speaks of a "rectification" instead of a "ratchet". The resulting peculiarities of the current-voltage characteristics of Josephson junctions can be observed experimentally. In the simple cases the agreement of theory and experiment is rather good: in [11] it has been demonstrated that the current-voltage curves, theoretically predicted basing on the overdamped dynamics model, coincide with the experimental data (see [12–14]). Recently, these investigations have been extended to the dynamics of arrays and ladders of Josephson junctions [15].

In this paper we consider an overdamped Josephson junction under the influence of an external quasiperiodic two-frequency driving. Due to the overdamped dynamics, chaos cannot be observed in this system. However, similar to other quasiperiodically forced systems, two possible dynamical regimes can be expected depending on parameter values, namely the quasiperiodic motion on a torus and the strange nonchaotic behavior. Thus, the dynamical

[a] e-mail: eireen@stat.physik.uni-potsdam.de

[1] This means that in this state there is no supercurrent flowing through the junction and the state is resistive.

regime with the highest possible complexity corresponds to the appearance of strange nochaotic attractors (SNAs). SNAs have been first described by Grebogi *et al.* [16] and since then investigated, both theoretically [17] and experimentally [18]. They share properties of regular as well as of chaotic attractors. Their geometrical structure is fractal like that of typical chaotic attractors, but they are not sensitive to initial conditions, because the non-trivial Lyapunov exponents of typical trajectories are negative. We will demonstrate that the appearance of a SNA can change drastically the current-voltage characteristics of the junctions. Therefore, we first study in detail the regions of quasiperiodic motion and strange nonchaotic behavior in the parameter space, and the transition phenomena between both these possible dynamical regimes. To distinguish between tori and SNA we suggest two methods, first one is based on their different geometrical structure and the second one on their spectral properties. Furthermore, we are interested in the transport phenomena and address the question how the transport (the current-voltage characteristics) depends on the existing dynamical regime and on the symmetry properties of the driving field and of the potential. To this end, we will discuss general symmetry properties for an overdamped particle in a spatially one-dimensional periodic potential under the influence of a two-frequency quasiperiodic driving field.

The paper is organized as follows. In Section 2 we introduce the equations of the quasiperiodically driven Josephson junction. In the following Section 3 we investigate the dynamical behavior in dependence on the parameter values and present a method to distinguish numerically between tori and SNAs. Then we suggest to use the spectral properties as a tool to determine the kind of the dynamics experimentally. For both possible dynamical regimes the current-voltage characteristics is discussed in Section 5. In Section 6 we consider general equations of motion and their symmetries. The undertaken symmetry considerations are used in Section 7 to find the conditions for the existence of a nonzero mean voltage across the junction. The results are summarized in Section 8, where we also discuss possible experimental implications.

2 Equations of motion

2.1 Overdamped junction

In order to derive the equation of motion we base on the Resistively Shunted Junction (RSJ) model [11], where the ideal Josephson junction (the supercurrent) is shunted parallely by a resistor and a capacity. Thus, the current components to be taken into account are the supercurrent, the normal current, and the displacement current. The supercurrent $I_S = I_C \sin(X)$ with maximal amplitude I_C is a function of the phase difference (Josephson phase) X of both condensate wave functions. Then, the basic equation describing the time evolution of the Josephson phase X according to the RSJ model is given by

$$\omega_p^{-2}\ddot{X} + \omega_c^{-1}\dot{X} + \sin(X) = i(t), \quad i(t) = I(t)/I_C, \qquad (1)$$

where $\omega_p = (2eI_C\hbar^{-1}C^{-1})^{1/2}$ is the junction plasma frequency and $\omega_c = 2eI_CR/\hbar$ is the characteristic frequency. The external current $I(t)$ is normalized with respect to the maximal amplitude I_C of the supercurrent. The dynamics of the junction is determined by the value of the dimensionless McCumber parameter $\beta = (\omega_c/\omega_p)^2$ which measures the strength of the damping or the capacitance effect. In the high damping limit $\beta \to 0$ with rescaling time $\tau = \omega_c t$ equation (1) simplifies to

$$\dot{X} + \sin(X) = i(t). \qquad (2)$$

This model of the dynamics of the overdamped Josephson junction will be considered throughout this paper. The variation of the Josephson phase is related to the voltage across the junction according to the so called phase-voltage relation

$$\dot{X} = \frac{2e}{\hbar}V. \qquad (3)$$

As can be read out from equation (3), a non-zero mean velocity $\langle\dot{X}\rangle$ just corresponds to a non-zero mean voltage $\langle V\rangle$ across the junction.

2.2 Mechanical analogs

Equation (2) describing the dynamics of the overdamped Josephson junction has important mechanical analogs. In the context of transport phenomena the most interesting is the one of the overdamped particle moving along the coordinate X with velocity $\dot{X}$ in a periodic potential $U(X) = -\cos(X)$, driven by an external force $i(t)$. According to the phase-voltage relation (3), the occurence of a mean voltage across the junction can be interpreted as a nonzero mean velocity of the particle, *i.e.* as a directed transport. Another mechanical analog is a plane mechanical pendulum in a uniform gravity field. Here, X is the angle of the deviation from the equilibrium of the pendulum, $\dot{X}$ is the angular velocity, and the current $i(t)$ corresponds to the torque.

2.3 Quasiperiodically driven Josephson junction

We are going to investigate now the dynamics of system (2) under the influence of a quasiperiodic driving field. Therefore, below the external driving term $i(t)$ will be an external field with zero mean, characterized by two incommensurate frequencies. While we write the equations in the most general form in Section 6 (see (8)), here we investigate a particular form that reads

$$\begin{aligned} \dot{X} &= F(X,\varphi_1,\varphi_2) \\ &= -\sin(X) + b_1\sin(\varphi_1) + b_2\sin(\varphi_2), \\ \dot{\varphi}_1 &= \omega_1, \\ \dot{\varphi}_2 &= \omega_2, \end{aligned} \qquad (4)$$

where $b_1,\ b_2$ are constant amplitudes of the components of the external driving field at frequencies ω_1 and ω_2. The

driving frequencies are chosen to be $\omega_1 = 1$ and $\omega_2 = \omega_1(\sqrt{5}-1)/2$. Their ratio is irrational, and is here fixed to be the inverse of the golden mean $\omega = \omega_2/\omega_1 = (\sqrt{5}-1)/2$, thus the external driving is quasiperiodic. There exist two trivial zero Lyapunov exponents connected with phases φ_1 and φ_2 of the quasiperiodic driving, and only one non-trivial Lyapunov exponent connected with the Josephson phase X. Because the divergence of the phase space volume is non-positive, the only non-trivial Lyapunov exponent has to be less than or equal to zero. Thus, it is impossible to observe chaos in the system.

3 Dynamical regimes

3.1 Constructing the Poincaré map

We are interested in the qualitative features of the dynamics: whether a quasiperiodic motion on a torus or a strange nonchaotic behavior occurs. Therefore, it is convenient to consider only a stroboscopic representation of the dynamics using periodicities inherent in the external field. We produce a series of X values by looking at the system only if the phase $\varphi_1 = \omega_1 t$ fulfils the condition $\varphi_1 \mod 2\pi = 0$. Using this stroboscopic method we obtain a series of X values discretized in time: $X(T_1),\ X(2T_1),\ X(3T_1), \cdots$, where T_1 is the period corresponding to the frequency ω_1, $T_1 = 2\pi/\omega_1$. Simultaneously, we trace the phase ϕ_2 at the same moments of time, producing the series $\theta_n = \phi_2(nT_1) \pmod{2\pi}$. The time evolution of the resulting phase variable θ is given by the phase shift $\theta_{n+1} = \theta_n + 2\pi\omega \pmod{2\pi}$. Now it is possible to draw the attractors on the Poincaré section (X, θ).

An important quantity to be calculated from the numerical solution of (4) is the mean velocity $\langle \dot{X} \rangle$. Because of the quasiperiodicity of the forcing, suitable for accurate numerics finite-time approximations read

$$\langle \dot{X} \rangle = \lim_{n\to\infty} \frac{X(F_n T_1) - X(0)}{F_n T_1}, \qquad (5)$$

where F_n is a Fibonacci number of possibly high level n. The Fibonacci numbers are defined by $F_0 = 0,\ F_1 = 1,\ F_2 = 1,\ F_{n+1} = F_n + F_{n-1}$.

3.2 Geometrical characterization of the dynamics

As has been already mentioned above, in dependence on the parameter values b_1 and b_2 two different dynamical regimes, namely torus and SNA can be observed. In general, there can be two types of torus in the system (4), depending on the mean value of $\langle \dot{X} \rangle$ (rotation number in X direction). If this rotation number is in rational relation with ω_1, ω_2, *i.e.* $\langle \dot{X} \rangle = \frac{p_1}{q_1}\omega_1 + \frac{p_2}{q_2}\omega_2$, then one speaks on 2-torus; it is represented by an attractive curve on the Poincaré map. If $\langle \dot{X} \rangle$ is not in rational dependence with ω_1, ω_2, one speaks on 3-torus, the trajectory in this case fills the whole phase space and all three Lyapunov exponents are zero [19]. Below we study the parameter values, for which no 3-tori occur, and hereafter "torus" means "2-torus".

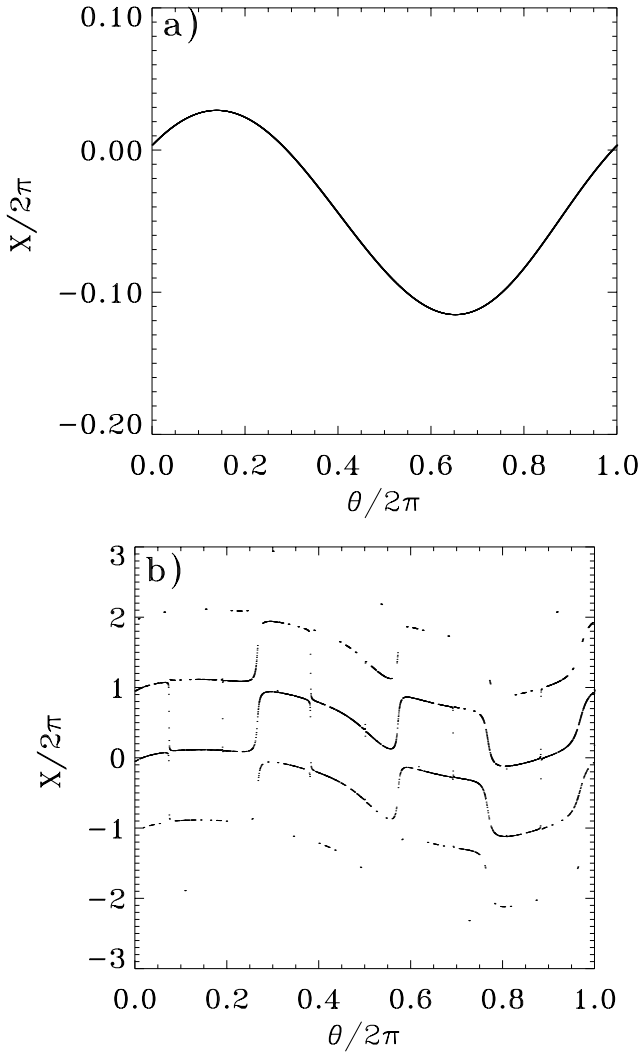

Fig. 1. Examples for the possible dynamical regimes for the system (4); (a) torus for $b_1 = b_2 = 0.5$, and (b) SNA for $b_1 = b_2 = 2.0$.

Figures 1a and b show an example for the torus and the SNA, respectively. Both regimes are characterized by negative nontrivial Lyapunov exponents, but differ obviously in their geometrical structure. In the case of torus shown in Figure 1a X is a smooth function of phase θ, whereas the attractor corresponding to the strange nonchaotic behavior (Fig. 1b) has a fractal structure.

How to distinguish between both regimes? Here we present a method based on the direct utilization of their different geometrical structures. Looking at Figure 1b more precisely one notes that the geometrical structure of the SNA is characterized by jumps of approximately $\pm 2\pi$ with respect to X values. Therefore, one should observe whether X values change much inside a small θ-interval. To this end, it is helpful to define a threshold inside which X values of closely neighboring θ values may differ from each other. This threshold can only be defined

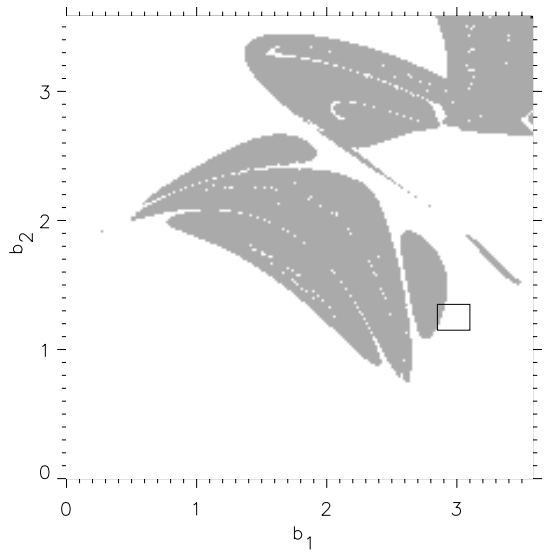

Fig. 2. Dynamical regimes (grey: SNA, white: torus) in the parameter plane (b_1, b_2) of the system (4) detected by using the geometrical approach described in the text. The little box is presented enlarged in Figure 3.

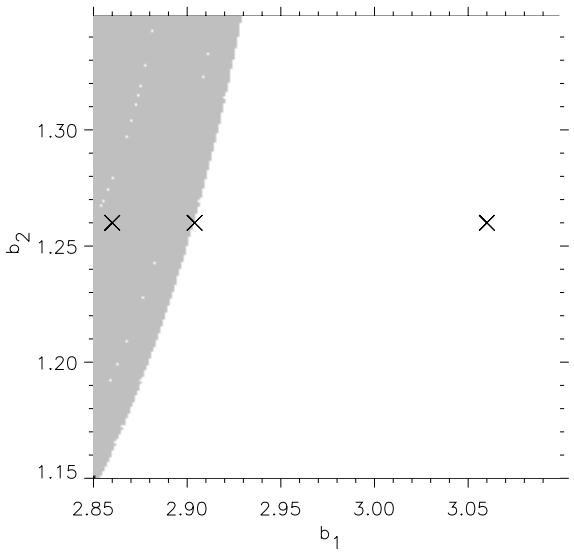

Fig. 3. Enlargement of the box in Figure 2 showing the dynamical regimes (grey: SNA, white: torus) in the parameter plane (b_1, b_2). The crosses denote the positions on the parameter plane ($b_2 = 1.26$, $b_1 = 3.06$, $b_1 = 2.904$, $b_1 = 2.86$) for which the attractors are presented in Figure 4.

on the basis of considering a sample of SNAs and tori and it is a choice valid for the special kind of system only. For the present system the threshold is given by 2π. In the case when the values of $|X|$ differ by a value larger than 2π within a small θ interval, the dynamical regime is a SNA. A torus is observed if the presence of a SNA can be excluded, *i.e.* if the absolute values of X do not differ by magnitudes $\geq 2\pi$ for θ values inside a small interval.

3.3 Parameter plane arrangement and fractal tori collision

Using the just described geometrical approach, the dynamical regimes of system (4) in dependence on the parameter values b_1 and b_2 in the range $[0, 3.6] \times [0, 3.6]$ have been estimated (Figs. 2 and 3). For particular parameter values marked by crosses in Figure 3 we present the attractor and the repeller (*i.e.* the attractor in system (4) solved backward in time) in the Poincaré section (Fig. 4). On one hand Figure 4 shows the attractors, but on the other hand also one of the possible mechanisms leading to the appearance of SNA, namely the collision of stable and unstable invariant tori in a dense set of values of phase θ but not in every value of θ [20]. The stable and unstable invariant sets in (4) have been computed by integrations forward and backward in time, respectively. In the Poincaré section we obtain stable and unstable tori for white regions of Figure 2. Coming closer to grey regions of the existence of the SNA by varying one of the parameters b_1 and b_2, or both, the stable and unstable tori become more wrinkled and come closer to each other (Figs. 4a,b). Finally they touch in a dense set of θ values but not at every value of the phase θ. As a result of this fractal tori collision a strange nonchaotic attractor appears (Fig. 4c).

4 Spectral properties

In experiment the distinction between both dynamical regimes could be done by considering the autocorrelation function (ACF) and the power spectrum. Note, that we refer in the following to the time-continuous process to estimate the spectral properties, whereas the discretized dynamics obtained by the Poincaré-section method is used to plot the attractors.

In the case of SNA we have observed a diffusion of the trajectory through the phase space. Thus, the time series $X(t)$, considered in the unbounded domain $-\infty < X < \infty$, is non-stationary. Therefore, we turn to another observable, namely $\sin(X)$, which is stationary in time, and investigate its spectral properties. For the Josephson junction this is the superconducting current. For consistency, we do the same for the case of torus although stationarity can be assumed here. The time series $\sin(X)$ corresponding to the torus shown in Figure 1a is represented in Figure 5a. As is well known, the autocorrelation function (ACF) of this quasiperiodic process is quasiperiodic, too (see Fig. 5b). Its main peaks return to value 1 and subsequent time differences between main peaks are equal to the product of the subsequent Fibonacci numbers and the period T_1, $\Delta_n = F_n T_1$. The power spectrum (Fourier transform) has peaks at the frequencies $f_1 = \omega_1/2\pi \approx 0.159$ and $f_2 = \omega_2/2\pi \approx 0.0983$, corresponding to the driving frequencies, and their harmonics (some of them are marked in Fig. 5c).

The time series $\sin(X)$ of the process generated by the SNA in Figure 1b is shown in Figure 6a. It has a more complex time dependence compared to the case of torus. This will be reflected in its spectral properties. The autocorrelation function of this process is represented in Figure 6b. The time axis is shown in a logarithmic scale to reveal

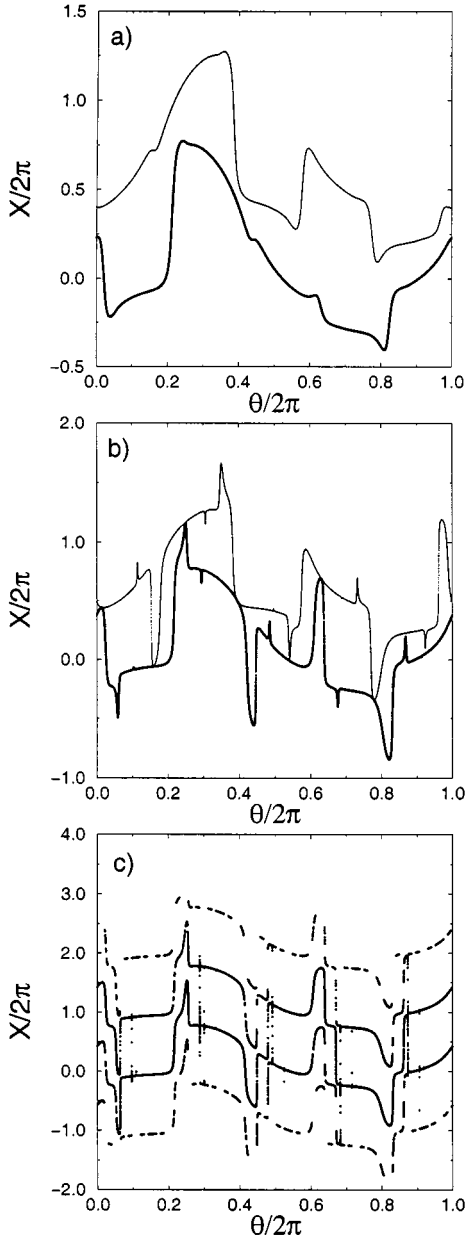

Fig. 4. The visualization of the fractal torus collision bifurcation (bold dots denote the stable torus and small dots the unstable one), where $b_2 = 1.26$ and (a) $b_1 = 3.06$, (b) $b_1 = 2.904$, (c) $b_1 = 2.86$. With decreasing parameter b_1 the stable and unstable curve become more wrinkled and come closer to each other and finally touch in a dense set of θ values but not in all values of θ. The result of this nonsmooth torus collision bifurcation is a SNA (c).

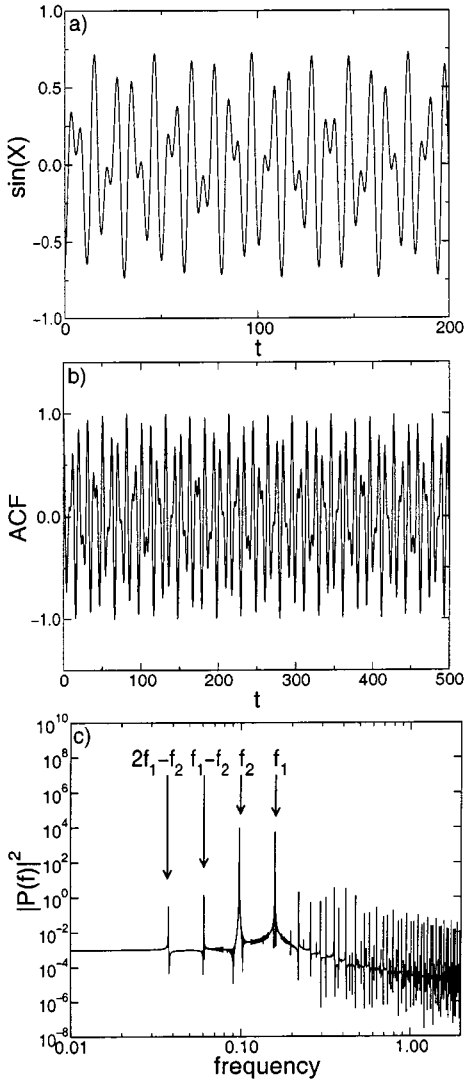

Fig. 5. The quasiperiodic time series $\sin(X)$ (a) corresponding to the torus shown in Figure 1a, its autocorrelation function (ACF) (b), and spectrum (c).

the self-similar structure of the ACF. In this representation we observe equidistant main peaks which are related again to Fibonacci numbers, being an indicator that the ratio of the driving frequencies is equal to the inverse of the golden mean. We observe that the main peaks return close to the value 1, what means that the disorder here is rather weak. Figure 6c shows the power spectrum of the process. We hypothesize that it is a mixture of a singular continuous and discrete spectrum [21]. A singular continuous spectrum sits on a set of Lebesgue measure zero and the peaks are weaker than δ functions. This type of spectrum is intermediate between discrete and continuous spectrum. Discrete spectrum is represented by δ-peaks and corresponds to a regular motion. Systems showing a chaotic behavior are characterized by a continuous spectrum. The singular continuous spectrum which one obtains in the case of SNA lies in between of these cases.

5 Current-voltage characteristics

In this section we are going to investigate the current-voltage characteristics in dependence on the observed dynamical regimes. As can be read out from equation (3), the velocity of the particles in the periodic potential corresponds to the voltage across the junction ($\dot{X} \sim V$).

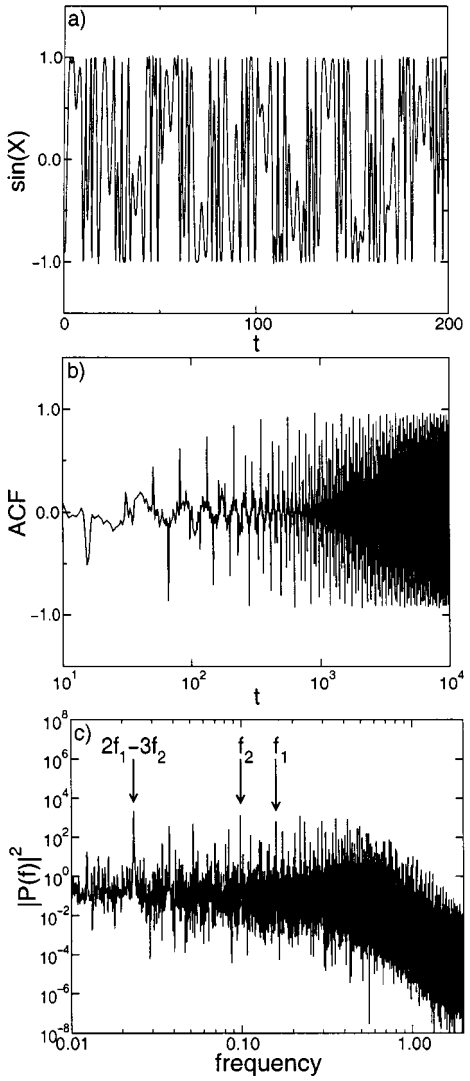

Fig. 6. The time series $\sin(X)$ (a) related to the SNA presented in Figure 1b, its autocorrelation function (b), and spectrum (c).

In order to discuss the current-voltage curve of the overdamped Josephson junction we need to modify the differential equation

$$\begin{aligned} \dot{X} &= -\sin(X) + I + b_1 \sin(\varphi_1) + b_2 \sin(\varphi_2), \\ \dot{\varphi}_1 &= \omega_1, \\ \dot{\varphi}_2 &= \omega_2, \end{aligned} \tag{6}$$

where the constant dc current I is introduced. Now it is possible to compute the current-voltage characteristics, namely to compute the mean velocity $\langle \dot{X} \rangle$ of the particle, or in terms of the Josephson junction theory the mean voltage across the junction, in dependence on the strength of current I. In the three cases below we always start with a certain dynamical regime for $I = 0$, and then investigate what happens for $I \neq 0$.

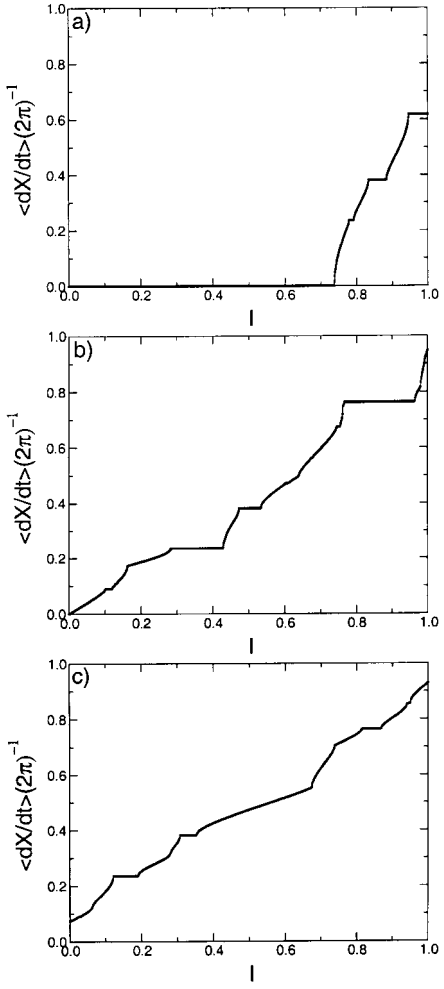

Fig. 7. The current-voltage characteristics ($\langle \mathrm{d}X/\mathrm{d}t \rangle \sim V$) for the system described by equation (6) (panels (a) and (b)), and for the system described by equation (7) (panel (c)). For (a) the regime of torus is obtained for parameter values $b_1 = b_2 = 0.5$, for (b) the regime of SNA for $b_1 = b_2 = 2.0$. Panel (c) shows the current-voltage curve for broken symmetry of the quasiperiodic driving function for the regime of SNA obtained for parameter values $b_1 = b_2 = c = 2.0$. In the case of SNA a broken symmetry yields a non-zero mean voltage along the junction (panel (c)) whereas for the case of torus inside some interval a supercurrent flows through the junction.

5.1 Torus

For the parameter values $b_1 = b_2 = 0.5$ and $I = 0$ the observed dynamical regime is torus. The current-voltage curve has been calculated using (5, 6) and is presented in Figure 7a. There exists some interval of I values for which the mean voltage across the junction is zero. This situation just represents the existence of a supercurrent flowing through the junction without any resistance. In the dynamical language, the ends of the interval correspond to points in the parameter space where stable torus – unstable torus collisions take place leading to the appearance of a SNA or of a 3-torus [22]. (We remind that

in order to compare with experiments, one has to multiply these dimensionless values with the critical current I_C.)

5.2 Symmetric SNA

System (6) demonstrates the SNA for $b_1 = b_2 = 2.0$ and $I = 0$. Figure 7b shows the current-voltage curve for these forcing amplitudes. In contrast to the case of the dynamical regime of torus the plateau at $\langle \dot{X} \rangle = 0$ is destroyed. Although $V = 0$ for $I = 0$, there is a finite slope $\frac{\mathrm{d}V}{\mathrm{d}I}\big|_{I=0}$. This state can be characterized as a resistive one. The observed plateaus at non-zero values of $\langle \dot{X} \rangle$ are so-called Shapiro steps [24,25]. The dynamical reason for the destruction of the superconducting state with $V = 0$ is the appearance of the unbounded fluctuations of X (see Fig. 4c). With any small dc-current I these fluctuations lead to a directed transport, what means finite resistance. In Section 3.2 we have established that the fractal structure of the SNA is characterized by jumps of the trajectory by $\pm 2\pi$. Thus, the probability to find jumps by $\pm 2\pi$ is non-zero. As long as the probability of occurence of jumps by $+2\pi$ is the same as of jumps by -2π the mean voltage across the junction is zero. This situation is changed if the external dc current I is nonzero: the probabilities of jumps are different, the jumps are biased and a finite voltage appears.

5.3 Asymmetric SNA

Of course, in general the quasiperiodic driving term can contain additional terms with combinations of both phases like in the following particular example

$$\begin{aligned} \dot{X} &= -\sin(X) + I + b_1 \sin(\varphi_1) + b_2 \sin(\varphi_2 + 2\pi/5) \\ &\quad + c \sin(\varphi_1 + \varphi_2 + \pi/4), \\ \dot{\varphi}_1 &= \omega_1, \\ \dot{\varphi}_2 &= \omega_2. \end{aligned} \tag{7}$$

Strange nonchaotic dynamical behavior for $I = 0$ can be found for $b_1 = b_2 = c = 2.0$. The corresponding current-voltage curve is presented in Figure 7c. As expected for the case of SNA, the state with $I \neq 0$ is resistive: the plateau of zero voltage $\langle \dot{X} \rangle = 0$ is destroyed. Moreover, we observe a non-zero voltage for $I = 0$ (and $I \neq 0$ for zero voltage across the junction). In the terms of general transport theory this means a ratchet or a rectification [10,23], *i.e.* a directed transport caused by a field whose mean value is zero. In the next two sections we will show that by including the third term in the quasiperiodic driving force (7) we have destroyed a certain symmetry with respect to phases φ_1 and φ_2. The asymmetry of the driving function leads in the case of SNA to a non-zero mean voltage across the junction.

6 General quasiperiodically driven systems and their symmetries

In this section we consider general quasiperiodically driven systems of the type

$$\begin{aligned} \dot{X} &= F(X, \varphi_1, \varphi_2) = -f(X) + E(\varphi_1, \varphi_2), \\ \dot{\varphi}_1 &= \omega_1, \\ \dot{\varphi}_2 &= \omega_2, \end{aligned} \tag{8}$$

where the ratio of frequencies ω_2/ω_1 is irrational and $E(\varphi_1, \varphi_2)$ is 2π-periodic in each argument. The function f is bounded and 2π-periodic: $f(X + 2\pi) = f(X)$.

Now, we intend to find out under which symmetry properties of the external field E and of the function f a non-zero current corresponding to non-zero mean velocity (5) can be observed. To this end, we are looking for symmetry transformations that leave the equations invariant. Here, we define transformations of the phase space X, φ_1 and φ_2 changing the sign of the average velocity $\langle \dot{X} \rangle$. Obviously, to transform the space we just carry out a reflection in $X \to -X$ (it may also be a reflection with respect to some point $X \to 2\mathcal{X} - X$, below we assume $\mathcal{X} = 0$ for clarity of presentation). We call $f(X)$ possessing $\hat{f}_a$ symmetry if $f(X)$ is antisymmetric. Next, we have to define transformations of the phases φ_1 and φ_2 in such a way that the equation of motion (8) remains unchanged under these transformations. As the symmetry property of function $E(\varphi_1, \varphi_2)$ we demand that it changes its sign after applying an appropriate phase shift (what is equal to any odd multiple of π) to one or both phases. Let us expand $E(\varphi_1, \varphi_2)$ into a Fourier series

$$E(\varphi_1, \varphi_2) = \sum_{k,l} E_{k,l} \exp(\mathrm{i}(k\varphi_1 + l\varphi_2)). \tag{9}$$

(Note that $E_{0,0} = I$ in our previous notation, we assume it to vanish). Considering the possible phase shifts of the phases φ_1 and φ_2 by π, we can distinguish three possible cases of phase shift symmetry:

1. Shift only phase φ_1 by π: $\varphi_1 \to \varphi_1 + \pi$, $\varphi_2 \to \varphi_2$ yields in the Fourier representation to

$$\begin{aligned} E(\varphi_1 + \pi, \varphi_2) &= \sum_{k,l} E_{k,l} \exp(\mathrm{i}(k\varphi_1 + l\varphi_2)) \exp(\mathrm{i}k\pi) \\ &= \sum_{k,l} (-1)^k E_{k,l} \exp(\mathrm{i}(k\varphi_1 + l\varphi_2)). \end{aligned}$$

   The function E changes its sign if k is odd while l can be chosen arbitrarily. It means that even harmonics with regard to phase φ_1 are forbidden. We call E possessing $\hat{E}_{S_1}$ symmetry if it changes its sign after applying a shift by π to phase φ_1:

$$E(\varphi_1 + \pi, \varphi_2) = -E(\varphi_1, \varphi_2). \tag{10}$$

2. Analogously, we call E possessing $\hat{E}_{S_2}$ symmetry if it changes its sign after applying a shift by π to phase φ_2:

$$E(\varphi_1, \varphi_2 + \pi) = -E(\varphi_1, \varphi_2). \tag{11}$$

3. Shift both phases by π: $\varphi_1 \to \varphi_1 + \pi$, $\varphi_2 \to \varphi_2 + \pi$. In the Fourier representation one obtains

$$\begin{aligned} & E(\varphi_1+\pi,\varphi_2+\pi) \\ &= \textstyle\sum_{k,l} E_{k,l} \exp(\mathrm{i}(k\varphi_1 + l\varphi_2)) \exp(\mathrm{i}(k+l)\pi) \\ &= \textstyle\sum_{k,l} (-1)^{k+l} E_{k,l} \exp(\mathrm{i}(k\varphi_1 + l\varphi_2)). \end{aligned}$$

The function E changes its sign if $k+l$ is an odd number, in this case we call E possessing $\hat{E}_{S_3}$ symmetry:

$$E(\varphi_1+\pi,\varphi_2+\pi) = -E(\varphi_1,\varphi_2). \tag{12}$$

Based on the discussed properties of function $E(\varphi_1,\varphi_2)$ we can define now the three relevant symmetries of (8), these are

$$\begin{aligned} &\hat{S}_1 : X \to -X,\ \varphi_1 \to \varphi_1 + \pi,\ \varphi_2 \to \varphi_2, \\ &\hat{S}_2 : X \to -X, \varphi_1 \to \varphi_1,\ \varphi_2 \to \varphi_2 + \pi\ , \\ &\hat{S}_3 : X \to -X,\ \varphi_1 \to \varphi_1 + \pi,\ \varphi_2 \to \varphi_2 + \pi\ . \end{aligned}$$

These symmetry transformations $\hat{S}_1$, $\hat{S}_2$ and $\hat{S}_3$ leave (8) unchanged if functions f and E possess $\hat{f}_a$ and $\hat{E}_{S_1}$, or $\hat{E}_{S_2}$, or $\hat{E}_{S_3}$ symmetry, respectively. (Note that $\hat{E}_{S_1}$ and $\hat{E}_{S_2}$ are, in fact, equivalent.) The existence of these symmetries will be shown below to have consequences for the transport of the particle in the periodic potential or, correspondingly, for the value of the mean voltage across the junction.

7 Symmetry and transport

Here we apply the symmetry properties to calculation of a directed transport. Let us assume that the X values have converged to a single attractor in the phase space (X,φ_1,φ_2). On the attractor one can define an invariant probability measure which we write in terms of a probability density $P(X,\varphi_1,\varphi_2)$. We assume that the invariant measure is ergodic: this is known for quasiperiodic motion on the torus, and is highly plausible (although a rigorous proof is still absent) for even more irregular SNA. Thus, the time average $\langle \dot{X} \rangle_t$ over a trajectory originated from a typical initial condition is the same as the phase space average

$$\begin{aligned} \langle \dot{X} \rangle_t = \textstyle\int_{-\pi}^{\pi} \int_0^{2\pi} \int_0^{2\pi} P\ (X,\varphi_1,\varphi_2)(-f(X) \\ +E(\varphi_1,\varphi_2))\mathrm{d}X\mathrm{d}\varphi_1\mathrm{d}\varphi_2. \end{aligned} \tag{13}$$

Suppose that the system possesses one of the symmetry transformations $\hat{S}_1$, $\hat{S}_2$, and $\hat{S}_3$. Because we assume existence of a single attractor, a symmetry of the invariant measures follows, thus $P(X,\varphi_1,\varphi_2) = P(-X,\varphi_1+\pi,\varphi_2)$ for $\hat{S}_1$, $P(X,\varphi_1,\varphi_2) = P(-X,\varphi_1,\varphi_2+\pi)$ for $\hat{S}_2$, and $P(X,\varphi_1,\varphi_2) = P(-X,\varphi_1+\pi,\varphi_2+\pi)$ for $\hat{S}_3$.

Now we calculate the value of the mean velocity of the $\hat{S}_1$–transformed phase space $\hat{S}_1(\langle \dot{X} \rangle_t) = \langle \dot{X} \rangle_t^{\hat{S}_1}$. It is given by

$$\begin{aligned} \langle \dot{X} \rangle_t^{\hat{S}_1} = \textstyle\int_{-\pi}^{\pi} \int_0^{2\pi} \int_0^{2\pi} P\ (-X,\varphi_1+\pi,\varphi_2)(-f(-X) \\ +E(\varphi_1+\pi,\varphi_2)\mathrm{d}X\mathrm{d}\varphi_1\mathrm{d}\varphi_2\ . \end{aligned} \tag{14}$$

Using the symmetry properties of the probability density P and of the functions f and E we can transform the integral:

$$\begin{aligned} \langle \dot{X} \rangle_t^{\hat{S}_1} &= \textstyle\int_{-\pi}^{\pi} \int_0^{2\pi} \int_0^{2\pi} P(-X,\varphi_1+\pi,\varphi_2)(-f(-X) \\ &\qquad +E(\varphi_1+\pi,\varphi_2)dXd\varphi_1d\varphi_2 \\ &= \textstyle\int_{-\pi}^{\pi} \int_0^{2\pi} \int_0^{2\pi} P(X,\varphi_1,\varphi_2)(f(X) \\ &\qquad -E(\varphi_1,\varphi_2))dXd\varphi_1d\varphi_2 \\ &= -\textstyle\int_{-\pi}^{\pi} \int_0^{2\pi} \int_0^{2\pi} P(X,\varphi_1,\varphi_2)(-f(X) \\ &\qquad +E(\varphi_1,\varphi_2))\mathrm{d}X\mathrm{d}\varphi_1\mathrm{d}\varphi_2 \\ &= -\langle \dot{X} \rangle_t. \end{aligned} \tag{15}$$

We conclude that the mean velocity of the transformed phase space and the velocity of the original one have the same absolute value and different signs. As we have assumed the existence of a single attractor that is transformed onto itself, this yields

$$\langle \dot{X} \rangle = -\langle \dot{X} \rangle_t = 0. \tag{16}$$

One can show similarly that (16) is also valid for symmetry transformations $\hat{S}_2$ and $\hat{S}_3$. In conclusion, for a single attractor in the phase space the current is zero if the fields f and E possess $\hat{f}_a$ and $\hat{E}_{S_1}$, or $\hat{E}_{S_2}$, or $\hat{E}_{S_3}$ symmetry, respectively. If no one of these symmetries of function E exists, or the antisymmetry of the space periodic function f is broken, we cannot derive the value of the mean velocity. In general, it can be expected not to vanish. In the case of torus, no matter which symmetry properties of the field f and E are present, it also vanishes for small non-symmetric perturbations, not leading to torus destruction. Another possibility is that there are two attractors A_1 and A_2, such that $\hat{S}_1(A_1) = A_2$. In this case of bistability the transport on each attractor is not vanishing, but it vanishes if we average over them with weights 1/2.

We are going now to consider the examples (6) and (7) from the point of view of the symmetry considerations. Let us first turn to equation (6). For zero current I equation (6) reduces to equation (4). As can be easily proved, there exist a special symmetry property of the equation (4) with respect to symmetry transformations in phase space. Applying the transformations: inverting the space $X \to -X$, and shifting the phases $\varphi_1 \to \varphi_1 + \pi$, $\varphi_2 \to \varphi_2 + \pi$ we establish that it remains unchanged under this symmetry transformation. These symmetry transformations are described by the $\hat{f}_a$ symmetry of function f and the $\hat{S}_3$ symmetry of the quasiperiodic driving field. For both dynamical regimes, torus and SNA, the numerically calculated mean velocity is zero. Now, the additional nonzero parameter I (see Eq. (6)) breaks the symmetry of the equation of motion, it means it is not invariant under

applying the symmetry transformations. However, it has no influence on the value of the mean voltage obtained for the regime of torus. It remains zero inside some interval for I values because the values of X are bounded. In other words, a particle whose motion is restricted to one cell of a periodic potential cannot be easily moved to the neighboring cell, one needs a finite force to allow for hoppings from cell to cell. The motion is asymmetric but remains bounded. In contrast to this, for the case of SNA where the values of X are unbounded, the broken symmetry, arising for non-zero value of I, causes a nonzero value for the mean voltage. Indeed, the unbounded values of X mean that a particle performs an unbiased random walk hopping from time to time to neighboring cells, and already a small breaking of symmetry produces a biased walk with nonzero mean voltage.

Considering now equation (7), we notice that it belongs to the set of systems for which the Fourier transform of function E contains terms $\exp(\mathrm{i}(k\varphi_1 + l\varphi_2))$ where $k + l$ is even, what destroys the $\hat{S}_3$ symmetry. Furthermore, no other symmetry transformations can be found such that the mean velocity changes the sign but equation (7) remains unchanged. Since the symmetry is broken for $I \neq 0$ as well as for $I = 0$, we expect that the current-voltage curve does not start in the origin of the current-voltage diagram but at some non-zero value of the mean voltage assuming the dynamical regime of SNA. This is confirmed by our computations of the current-voltage curve of (7) (see Fig. 7c).

8 Conclusion

In this paper we have considered the model of the overdamped Josephson junction under the influence of an external quasiperiodic driving field. The dynamics of this system can be either quasiperiodic (represented by a motion on a torus) or strange nonchaotic, in dependence on parameter values. We have applied a geometrical approach based on the different geometrical structure in Poincaré map to distinguish between the torus and the SNA. The analysis of the dynamical regimes has been supplemented by investigation of the spectral properties (autocorrelation function and power spectrum) which are accessible in experiments. For each dynamical behavior the current-voltage characteristics has been computed and discussed. It has been found out that the dc current breaks the symmetry of the equation of motion, what has consequences for the current-voltage curve in the case of SNA. Here a mean voltage develops across the junction, whereas for the regime of torus a supercurrent can flow through. Thus, the appearance of a SNA can be followed in experiments as the appearance of a resistive state at zero dc external current.

To prove the hypothesis that for the regime of SNA a broken symmetry leads to a non-zero mean voltage across the junction, we have considered general quasiperiodically driven overdamped dynamical systems and have analysed their symmetry properties. There exist three basic types of symmetry transformation changing the sign of the mean velocity but leaving the equation of motion unchanged. If the symmetries are broken, in general a non-zero current of the particle corresponding to a non-zero mean voltage could be observed. However, the type of the dynamical behavior plays an important role, too. Only in the case of SNA, where an unlimited diffusion of trajectories in the phase space occurs, a non-zero mean velocity can be observed already for small breaking of symmetries. In the case of tori, small asymmetries have no influence and the mean voltage remains zero inside a certain interval of the external dc current.

The work was supported by DFG. We thank S. Flach, P. Hänggi, S. Kuznetsov, P. Reimann, and A. Ustinov for illuminating discussions.

References

1. R. Lipowsky, Phys. Rev. Lett. **85**, 4401 (2000); O.M. Yevtushenko, K. Richter, Phys. Rev. B **57**, 14839 (1998); A.A. Abrikosov, *Fundamentals of the Theory of Metals* (North-Holland, Amsterdam, 1988).
2. *Lecture Notes in Physics: Stochastic Processes in Physics, Chemistry, and Biology*, edited by J.A. Freund, T. Pöschel (Springer, Berlin, 2000).
3. P. Hänggi, R. Bartussek, in *Nonlinear Physics of Complex Systems – Current Status and Future Trends*, Lecture Notes in Physics Vol. 476, edited by J. Parisi, S.C. Müller, W. Zimmermann (Springer, Berlin, 1996), pp. 294–308.
4. P. Reimann, Phys. Rev. Lett. **86**, 4992 (2001); P. Reimann, `arXiv: cond-mat/0010237`, submitted to Phys. Rep.
5. P. Jung, J. G. Kissner, P. Hänggi, Phys. Rev. Lett. **76**, 3436 (1996)
6. J.L. Mateos, Phys. Rev. Lett. **84**, 258 (2000).
7. S. Flach, O. Yevtushenko, Y. Zolotaryuk, Phys. Rev. Lett. **84**, 2358 (2000).
8. I. Goychuk, P. Hänggi, Europhys. Lett. **43**, 503 (1998).
9. O. Yevtushenko, S. Flach, Y. Zolotaryuk, A.A. Ovchinnikov, Europhys. Lett. **54**, 141 (2001); S. Flach, A.A. Ovchinnikov, Physica A **292**, 268 (2001); O. Yevtushenko, S. Flach, K. Richter, Phys. Rev. **61**, 7215 (2000).
10. I. Zapata, R. Bartussek, F. Sols, P. Hänggi, Phys. Rev. Lett. **77**, 2292, (1996); I. Zapata, J. Luczka, F. Sols, P. Hänggi, Phys. Rev. Lett. **80**, 829 (1998).
11. K.K. Likharev, *Dynamics of Josephson Junctions and Circuits* (Gordon and Breach Science Publishers, New York, 1981).
12. P.K. Hansma, G.I. Rochlin, J.N. Sweet, Phys. Rev. B **4**, 3003 (1971).
13. P.K. Hansma, G.I. Rochlin, J. Appl. Phys. **43**, 4721 (1972).
14. R.P. Giffard, P.F. Michelson, R.J. Soulen, Jr., IEEE Trans. Magn. **15**, 276 (1979).
15. E. Goldobin, A.V. Ustinov, Phys. Rev. B **59**, 11532 (1999); M.V. Fistul, P. Caputo, A.V. Ustinov, Phys. Rev. B **60**, 13152 (1999); D. Abraimov, P. Caputo, G. Filatrella, M.V. Fistul, G.Yu. Logvenov, A.V. Ustinov, Phys. Rev. Lett. **83**, 5354 (1999).
16. C. Grebogi, E. Ott, S. Pelikan, J.A. Yorke, Physica D **13**, 261 (1984).

17. A. Bondeson, E. Ott, T.M. Antonsen, Phys. Rev. Lett. **55**, 2103 (1985); F.J. Romeiras *et al.*, Physica D **26**, 277 (1987); F.J. Romeiras E. Ott, Phys. Rev. A **35**, 4404 (1987); M. Ding, C. Grebogi, E. Ott, Phys. Rev. A **39**, 2593 (1989); M. Ding, C. Grebogi, E. Ott, Phys. Lett. A **137**, 167 (1989); T. Kapitaniak, E. Ponce, J. Wojewoda, J. Phys. A **23**, L383 (1990); J.F. Heagy, S.M. Hammel, Physica D **70**, 140 (1994); A. Pikovsky, U. Feudel, J. Phys. A **27**, 5209 (1994); M. Ding, J. Scott Kelso, Int. J. Bif. Chaos **4**, 553 (1994); U. Feudel, J. Kurths, A. Pikovsky, Physica D **88**, 176 (1995); S. Kuznetsov, U. Feudel, A. Pikovsky, Phys. Rev. E **57**, 1585 (1998); Y.-C. Lai, Phys. Rev. E **53**, 57 (1996); T. Nishikawa, K. Kaneko, Phys. Rev. E **54**, 6114 (1996); T. Yalcinkaya, Y.-C. Lai, Phys. Rev. Lett. **77**, 5039 (1996); A. Prasad, V. Mehra, R. Ramaswamy, Phys. Rev. Lett. **79**, 4127 (1997); A. Prasad, V. Mehra, R. Ramaswamy, Phys. Rev. E **57**, 1576 (1998); A. Witt, U. Feudel, A. Pikovsky, Physica D **109**, 180 (1997).
18. W.L. Ditto *et al.*, Phys. Rev. Lett. **65**, 533 (1990); T. Zhou, F. Moss, A. Bulsara, Phys. Rev. A **45**, 5394 (1992); B. Bezruchko, S. Kuznetsov, Ye. Seleznev, Phys. Rev. E **62**, 7828 (2000).
19. U. Feudel, J. Kurths, A.S. Pikovsky, Physica D **88**, 176 (1995).
20. U. Feudel, C. Grebogi, E. Ott, Phys. Rep. **290**, 11 (1997).
21. A.S. Pikovsky, M.A. Zaks, U. Feudel, J. Kurths, Phys. Rev. E **52**, 285 (1995).
22. P. Glendinning, U. Feudel, A.S. Pikovsky, J. Stark, Physica D **140**, 227 (2000).
23. O. Yevtushenko, S. Flach, Y. Zolotaryuk, A.A. Ovchinnikov, Europhys. Lett. **54**, 141 (2001).
24. B.D. Josephson, Phys. Lett. **1**, 251 (1962).
25. S. Shapiro, A.R. Janus, S. Holly, Rev. Mod. Phys. **36**, 223 (1964).